Acta Crystallographica Section D
Biological Crystallography
ISSN 0907-4449

Lack of dynamics in the MabA active site kills the enzyme activity: practical consequences for drug-design studies

Guillaume Poncet-Montange,[a] Stephanie Ducasse-Cabanot,[b] Annaick Quemard,[b] Gilles Labesse[a] and Martin Cohen-Gonsaud[a]*

[a]CNRS UMR5048, Centre de Biochimie Structurale, F-34090 Montpellier, France; INSERM U554, F-34090 Montpellier, France; Université Montpellier I et II, F-34090 Montpellier, France, and [b]Institut de Pharmacologie et de Biologie Structurale, Département des Mécanismes Moléculaires des Infections Mycobactériennes, CNRS UMR5089, 205 Route de Narbonne, 31077 Toulouse CEDEX, France

Correspondence e-mail: martin@cbs.cnrs.fr

Received 26 March 2007
Accepted 16 May 2007

PDB Reference: MabA, 2ntn, r2ntnsf.

The MabA protein from *Mycobacterium tuberculosis* is a validated drug target. Previous structural studies of this protein showed dynamic behaviour in the catalytic site and described motion between an open 'active' holo form (with NADP) and a closed 'inactive' apo form (without NADP). Here, a mutation (G139A) is reported that leads to complete protein inactivation and freezes the catalytic site into its closed form, even in the presence of the cofactor. This observation suggests a new way to develop anti-MabA drugs *via* protein stabilization of the 'inactive' form.

1. Introduction

The mycolic acids are very long chain lipids that are essential to the bacterium *Mycobacterium tuberculosis*. The mycolic acid elongation system fatty acid synthetase II (FAS-II) is composed of four enzymes, all of which are confirmed drug targets (Mdluli & Spigelman, 2006). Indeed, two of the most important antituberculous drugs target this system (isoniazid and ethionamide). The MabA protein, a β-keto-acyl-acyl carrier protein β-ketoacyl-ACP reductase (KAR) encoded by the gene Rv1483, also named *fabG1*, catalyses the second step of FAS-II (Marrakchi *et al.*, 2002). Recently, it has also been shown to be essential, with only actinomycetal orthologues being able to complement its disruption (Parish *et al.*, 2007).

MabA has the short-chain dehydrogenase/reductase (SDR) fold observed in many oxidoreductases, but shows an unusual mobility in the catalytic site that has also been described for its *Escherichia coli* homologue KARec (Price *et al.*, 2001; Cohen-Gonsaud *et al.*, 2002) and more recently for an orthologue from *Streptomyces coelicolor* (Tang *et al.*, 2006). In the apo form several residues are not visible in the electron density, suggesting that the $\beta4/\alpha4$ (residues 90–99) and $\beta5/\alpha5$ (residues 142–149) regions are highly flexible. These regions are surrounded by residues that are important for activity, including two residues of the conserved catalytic triad: Ser140 and Tyr153.

In MabA and KARec (Price *et al.*, 2004), a 90° rotation of the catalytic tyrosine Tyr153 is observed and the catalytic serine Ser140 and valine Val141 move by 5 and 8 Å, respectively, between the apo form and the holo form ($C^{\alpha}-C^{\alpha}$ distance). This rearrangement brings the backbone of Ser140 and the side chain of Val141 into the positions that the ribose and the nicotinamide ring of NADP occupy in the holo form (Fig. 1). The terminology 'closed form' is used for the 'inactive' apo structure, while 'open form' is used for the 'active' holo structure. In the holo form of the related KARbn (KAR from *Brassica napus*; PDB code 1edo; Fisher *et al.*, 2000) the corresponding residues are well ordered, as in both the apo and holo forms of other SDRs.

In our previous structural studies, a double mutant C60V/S144L of MabA was used. This double-mutant protein enhances the stability during purification (C60V) and stabilizes the catalytic loop in its open 'active' form (S144L). We identified two unique structural features in the MabA crystal structures that were absent in the KARec structures. Firstly, if the $\beta5/\alpha5$ loop is structured in the holo structure then some density corresponding to the disordered loop of the apo structure is present (see PDB code 1uzn). As a consequence, the density for the cocrystallized cofactor is not fully present and the

Table 1
Data-collection and refinement statistics.

Values in parentheses are for the outermost resolution shell.

Space group	*C*2
Unit-cell parameters (Å, °)	a = 81.6, b = 117.3, c = 52.3, β = 121.9
No. of molecules in the ASU	2
Resolution range (Å)	27–2.3 (2.4–2.3)
Total reflections	45213
Unique reflections	17168
Redundancy	2.6
$R_{\rm merge}$† (%)	9.8 (36.5)
$I/\sigma(I)$	11.1 (3.0)
Completeness (%)	92.6 (95.4)
$R_{\rm work}$‡ (%)	17.7
$R_{\rm free}$§ (%)	23.8
R.m.s. deviations from ideal values	
Bond lengths (Å)	0.010
Bond angles (°)	1.2

† $R_{\rm merge} = \sum_{hkl}\sum_i |I_{hkl,i} - \langle I_{hkl}\rangle|/\sum_{hkl}\sum_i |I_{hkl,i}| \times 100$. ‡ $R_{\rm work} = \sum_{hkl} |F_{\rm obs} - F_{\rm calc}|/\sum_{hkl} |F_{\rm obs}| \times 100$. § $R_{\rm free} = \sum_{hkl} |F_{\rm obs} - F_{\rm calc}|/\sum_{hkl} |F_{\rm obs}| \times 100$ for 1030 reflections (6%).

nicotinamide moiety cannot be modelled (Cohen-Gonsaud *et al.*, 2005). Secondly, the stabilization of the catalytic loop is linked to the structuring of two other parts of the protein. The loops $\beta4/\alpha4$ and $\beta5/\alpha5$ become structured by the formation of three hydrogen bonds from residues of the same monomer. However, the most striking associated rearrangement appears in the C-terminal part of the protein (^{243}MGMGH^{247}). The residues of the four monomers of the biological unit, specific to the mycobacterial species, become structured and form a complex network of hydrogen bonds to the catalytic loops (Cohen-Gonsaud *et al.*, 2005).

As the cofactor was not entirely visible and as our attempt to obtain a tertiary complex of MabA with both the cofactor and a ligand failed, we tried to identify a mutation that would stabilize such a complex. The SDR sequences were again analysed to identify new determinants of flexibility within the catalytic loop. In both MabA and KARec a glycine is present at the end of $\beta5$ (Gly139 in MabA), while residues with larger side chains are present in the other SDRs (*i.e.* Ala153 in KARbn). A substitution of Gly139 by alanine was thus predicted to decrease the conformational dynamics observed in the apo form of the wild-type enzyme.

2. Materials and methods

Cloning, directed mutagenesis, purification, crystallization and steady-state kinetic experiments were performed as described previously (Cohen-Gonsaud *et al.*, 2002, 2005; Marrakchi *et al.*, 2002). The protein was checked by electrospray ionization mass spectroscopy (ESI-MS) and loss of the N-terminal methionine residue was observed. The data sets were collected in-house at cryogenic temperature using a Rigaku RU-200 rotating-anode X-ray generator (graphite-monochromated Cu $K\alpha$, λ = 1.5418 Å) and a MAR Research image-plate detector. New crystallization conditions were determined using a hanging-drop-based sparse-matrix screening strategy (Hampton Research kits). Protein crystals were grown in 5 d at room temperature by mixing 1 µl protein solution (with or without 5 m*M* NADP) and 1 µl crystallization buffer (100 m*M* Tris pH 8.0, 22% polyethylene glycol 2000, 350 m*M* magnesium acetate and 10% glycerol) and equilibrating against 0.5 ml of the same buffer. Prior to data collection, crystals were harvested with a nylon cryo-loop and immediately flash-cooled in liquid nitrogen. Image processing and data scaling were performed using the programs *MOSFLM*, *SCALA* and *TRUNCATE* from the *CCP*4 program suite (Collaborative Computational Project, Number 4, 1994) (Table 1). Isomorphous crystals were obtained and structure refinement was initiated by rigid-body minimization using the crystal structure of MabA-C60V. The graphics program *Coot* was used for manual rebuilding (Emsley & Cowtan, 2004). Structure refinement was performed using *REFMAC* 5.0 from the *CCP*4 package and after a few steps of rigid-body minimization, restrained refinement using maximum likelihood was applied. Several water molecules were added automatically using *ARP*/*wARP* (Morris *et al.*, 2003). TLS parameters (Winn *et al.*, 2001) were then applied. The details of the refinement statistics and model accuracy are listed in Table 1.

3. Results and discussion

Poor-quality crystals were initially obtained under similar crystallization conditions to those used for the wild-type or other mutant proteins. New conditions were subsequently found at a higher pH and without Cs^+ ions. However, no space-group or unit-cell parameter changes were observed for this new mutant. The best crystals obtained with and without cofactor diffract to a limit of 2.3 Å. Isomorphous replacement and manual rebuilding cycles with simulated annealing were performed and led to the final model.

To our surprise, the mutation G139A leads to stabilization of the catalytic loop in its closed form with unstructured C-terminal residues. Indeed, the structures that we solved from data collected from crystals grown in the presence or in the absence of the cofactor were identical (data not shown). With the S144L mutant, the presence of NADP in the crystallogenesis solutions always led to the the open conformation of the catalytic loop.

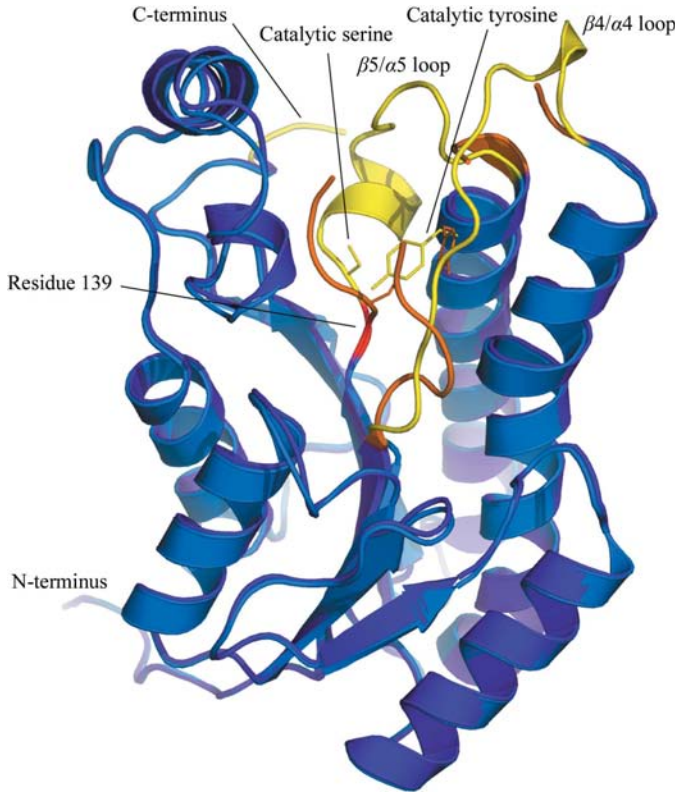

Figure 1
Superposition of the closed inactive form (in light blue) and the open active form (in dark blue). The catalytic Ser140 and Tyr153 are shown in stick representation. The rearranged regions of the protein are represented in yellow for the open form and orange for the closed form. Residue 139 is coloured red.

Steady-state kinetic experiments in the presence of acetoacetyl-CoA and NADPH were performed on the newly generated protein MabA-C60V/G139A/S144L. This triple mutant bearing an alanine instead of a glycine at position 139 appeared to be totally inactive. This suggested that the closed form observed in the crystal structure of the triple mutant is highly stable in solution and prevents the entrance of ligands into the active site.

In most prokaryotic KAR sequences a glycine is present at the position equivalent to the residue 139 of MabA, while in eukaryotic KARs and SDRs an alanine or a serine are present. The three prokaryotic KAR structures that have been solved (those from *E. coli*, *S. coelicolor* and *M. tuberculosis*) display the same rearrangement within the catalytic loop. An exclusively open form of the catalytic loop is observed in the related structures of eukaryotic homologues. We hypothesized that a transition state with φ/ψ angles that are compatible with a glycine but not with a serine or an alanine is necessary to switch between the open and a closed form.

With this point mutation we managed, surprisingly, to freeze the protein in its inactive form. We arrived at a situation in which the open active form is no longer accessible, leading to a totally inactive enzyme. This result opens new perspectives for drug-design studies. The 'classical' option is to inactivate the MabA protein with a ligand that fits inside the active site. This might lead to a difficult optimization in order to gain specificity over the the eukaryotic homologues. Instead of trying to identify such a competitive inhibitor, the prospect of finding a noncompetitive inhibitor that locks the protein in its closed and 'inactive' state may be a better option for future drug-design studies. As a consequence, the crystal structure of the inactive form (PDB code 2ntn) could be used in *in silico* and *in cristallo* screening for ligands that stabilize the catalytic loop in its closed inactive form.

References

Cohen-Gonsaud, M., Ducasse, S., Hoh, F., Zerbib, D., Labesse, G. & Quemard, A. (2002). *J. Mol. Biol.* **320**, 249–261.

Cohen-Gonsaud, M., Ducasse-Cabanot, S., Quemard, A. & Labesse, G. (2005). *Proteins*, **60**, 392–400.

Collaborative Computational Project, Number 4 (1994). *Acta Cryst.* D**50**, 760–763.

Emsley, P. & Cowtan, K. (2004). *Acta Cryst.* D**60**, 2126–2132.

Fisher, M., Kroon, J. T., Martindale, W., Stuitje, A. R., Slabas, A. R. & Rafferty, J. B. (2000). *Structure Fold. Des.* **8**, 339–347.

Marrakchi, H., Ducasse, S., Labesse, G., Montrozier, H., Margeat, E., Emorine, L., Charpentier, X., Daffe, M. & Quemard, A. (2002). *Microbiology*, **148**, 951–960.

Mdluli, K. & Spigelman, M. (2006). *Curr. Opin. Pharmacol.* **6**, 459–467.

Morris, R. J., Perrakis, A. & Lamzin, V. S. (2003). *Methods Enzymol.* **374**, 229–244.

Parish, T., Roberts, G., Laval, F., Schaeffer, M., Daffe, M. & Duncan, K. (2007). *J. Bacteriol.* **189**, 3271–3278.

Price, A. C., Zhang, Y. M., Rock, C. O. & White, S. W. (2001). *Biochemistry*, **40**, 12772–12781.

Price, A. C., Zhang, Y. M., Rock, C. O. & White, S. W. (2004). *Structure*, **12**, 417–428.

Tang, Y., Lee, H. Y., Kim, C. Y., Mathews, I. & Khosla, C. (2006). *Biochemistry*, **45**, 14085–14093.

Winn, M. D., Isupov, M. N. & Murshudov, G. N. (2001). *Acta Cryst.* D**57**, 122–133.